

# Design and Characterization of an Injectable Pericardial Matrix Gel: A Potentially Autologous Scaffold for Cardiac Tissue Engineering

Sonya B. Seif-Naraghi, B.S.E., Michael A. Salvatore, B.S., Pam J. Schup-Magoffin, B.A.,  
Diane P. Hu, M.S., and Karen L. Christman, Ph.D.

Following ischemic injury in the heart, little to no repair occurs, causing a progressive degeneration of cardiac function that leads to congestive heart failure. Cardiac tissue engineering strategies have focused on designing a variety of injectable scaffolds that range in composition from single-component materials to complex extracellular matrix (ECM)-derived materials. In this study, the pericardial ECM, a commonly used biomaterial, was investigated for use as an injectable scaffold for cardiac repair. It was determined that a solubilized form of decellularized porcine pericardium could be injected and induced to gel *in vivo*, prompting investigation with human pericardium, which has the decided advantage of offering an autologous therapy. Characterization showed that the matrix gels retained components of the native pericardial ECM, with extant protein and glycosaminoglycan content identified. The results of an *in vitro* migration assay indicate that the porcine pericardial matrix is a stronger chemoattractant for relevant cell types, but *in vivo* results showed that the two materials caused statistically similar amounts of neovascularization, demonstrating feasibility as injectable treatments. Potential stem cell mobilization was supported by the presence of c-Kit<sup>+</sup> cells within the matrix injection regions. With this work, the pericardium is identified as a novel source for an autologous scaffold for treating myocardial infarction.

## Introduction

CARDIOVASCULAR DISEASE CONTINUES to be the leading killer in the Western world, being responsible for 1 out of every 2.8 deaths in the United States.<sup>1</sup> Heart failure (HF) following a myocardial infarction (MI) accounts for a majority of these deaths.<sup>1</sup> Lacking significant regenerative capabilities, cardiac tissue is not repaired after ischemic injury,<sup>2</sup> leading to negative left ventricular (LV) remodeling and subsequent HF.<sup>3</sup> Currently, the only successful treatment for end-stage HF post-MI is total heart transplantation, a treatment severely limited by a dearth of donor hearts and the risk associated with such an invasive procedure. Recently, tissue engineering approaches are providing exciting new possibilities.

Treatments such as cellular cardiomyoplasty<sup>4,5</sup> and cardiac patches<sup>6,7</sup> have been investigated, but each faces limitations such as poor cell retention and survival with the former or an invasive surgical procedure with the latter. Thus, there is still a need for a minimally invasive solution that would mitigate negative LV remodeling, thereby preventing HF.

Recent cardiac tissue engineering approaches have focused on designing injectable scaffolds for use in cellular and acellular therapies.<sup>6,8</sup> An injectable scaffold provides the potential advantage of catheter delivery and, by gelling *in situ*, can provide a structural support that allows for cell infiltration to promote a repair or regenerative response, or act as a scaffold to prevent anoikis of transplanted cells. Investigated scaffold materials include fibrin,<sup>9,10</sup> collagen,<sup>11</sup> alginate,<sup>12</sup> chitosan,<sup>13</sup> self-assembling peptide nanofibers,<sup>14–16</sup> polyethylene glycol,<sup>17</sup> Matrigel<sup>™</sup>,<sup>18</sup> and an extracellular matrix (ECM) gel derived from decellularized porcine myocardium.<sup>8</sup> All of these materials are injectable, but only Matrigel and the myocardial matrix gel mimic the ECM with respect to complexity of biochemical composition, including proteins, peptides, and polysaccharides that comprise the native ECM. Matrigel, however, is limited in its clinical relevance since it is produced by mouse sarcoma cell lines, and while the most attractive aspect of the myocardial matrix gel is that it provides tissue-specific ECM cues, it is also necessarily xenogeneic.<sup>8</sup> Although not for the application of cardiac repair, a similar injectable matrix scaffold has been made from decellularized urinary bladder matrix.<sup>19</sup>

Porcine pericardium is another tissue commonly decellularized for use in various applications, conventionally used in glutaraldehyde-fixed bioprostheses. It is FDA approved for use in a variety of applications, including stent covers,<sup>20</sup> dural grafts,<sup>21</sup> prosthetic valve materials,<sup>22</sup> and in the repair of soft tissue defects.<sup>23–25</sup> As a fibrous sac chiefly composed of compact collagen layers interspersed with elastin fibers,<sup>26</sup> the pericardium is generally used for its mechanical properties and convenient shape. Historically, the tissue decellularized to make patches and grafts, or produce ECM gels has been necessarily xenogeneic or allogeneic,<sup>27</sup> as one's own small intestine submucosa, bladder, and cardiac tissue cannot be harvested in sizeable quantities without detriment. In contrast, a clinically attractive aspect of using pericardial tissue therapeutically is that the pericardium is not essential to life. No adverse consequences result from congenital absence or surgical resection.<sup>28</sup> During cardiothoracic surgery, the pericardium is routinely left unsutured when the procedure is complete, and removing a small piece of this tissue poses little health risk to the patient. Autologous pericardium has been utilized in cardiac surgery due to its ready availability, ease of handling, and low cost.<sup>29</sup> Applications have included mitral valve extension,<sup>30</sup> aortic valve replacement,<sup>29</sup> and even reconstruction of the left ventricle.<sup>31</sup>

Thus, if the endogenous repair shown with porcine scaffolds—including cell infiltration and neovascularization<sup>8,27,32,33</sup>—can be achieved using a scaffold derived from this autologous source, it would provide a faster route to clinical translation, reducing regulatory concerns, and avoiding any ethical, immunogenic, or disease transfer concerns associated with xenogeneic sources. In this work, the pericardium is identified as a potential source of autologous human ECM for use as an injectable cardiac tissue engineering scaffold.

The objectives of this study were to develop and characterize an injectable pericardium scaffold for cardiac tissue engineering applications. The techniques described herein were first established with healthy, juvenile porcine tissue, but, given the attractiveness of an autologous therapy, it was of interest to determine if the same were possible with demographically relevant human tissue, in this case, patients with cardiovascular disease undergoing cardiothoracic surgery. In this study, the biochemical composition, *in vitro* chemoattractant potential, and *in situ* cellular infiltration of two injectable ECM scaffolds derived from decellularized porcine and human pericardial tissue are reported, demonstrating feasibility of two novel pericardial ECM gels to serve as *in vivo* scaffolds for cell recruitment and indicating proof-of-concept for an autologous biomaterial treatment for the myocardium.

## Materials and Methods

All experiments in this study were performed in accordance with the guidelines published by the Institutional Animal Care and Use Committee at the University of California, San Diego, and the American Association for Accreditation of Laboratory Animal Care.

### Tissue collection

Porcine pericardium samples were harvested from juvenile farm pigs weighing approximately 45–50 kg. Animals

used for this purpose had previously been anesthetized with isoflurane and immediately before harvest were euthanized with an overdose of Pentobarbital (90 mg/kg) administered intravenously. Human pericardium samples were collected from consenting patients scheduled for cardiothoracic surgery; the surgeon removed a small piece (approximately 4–5 cm<sup>2</sup>) of tissue during surgery, in compliance with the University of California, San Diego, Institutional Review Board.

### Decellularization

After dissecting away any adherent adipose tissue, fresh porcine and human tissues were decellularized using hypotonic and hypertonic rinses in deionized (DI) water and sodium dodecyl sulfate (SDS), an ionic detergent previously shown to decellularize pericardium.<sup>34</sup> Specifically, the porcine pericardium was first washed in DI water for 30 min, and then stirred continuously in 1% SDS in phosphate-buffered saline (PBS) for 24 h, followed by a 5 h DI water rinse. All human pericardia were first washed in DI water for 30 min, and then stirred continuously in 1% SDS in PBS for 60–65 h, followed by an overnight DI rinse. For both types of tissue, specimens were then removed from solution and again rinsed under running DI water. A small piece was removed and fresh frozen in O.C.T. freezing medium, and 10  $\mu$ m tissue sections were taken every 100  $\mu$ m throughout the sample for verification of complete decellularization via histological analysis, as previously reported.<sup>34–36</sup> Briefly, hematoxylin and eosin (H&E) staining was performed, and the tissue was examined for the absence of nuclei. A fluorescent Hoechst 33342 stain (1.0  $\mu$ g/mL) for DNA was also performed to verify the H&E results; briefly, sections were fixed in acetone, rehydrated, rinsed in water, stained for 10 min, and then rinsed with PBS and stored in the dark.

### Preparation of solubilized ECM

Solubilized ECM was prepared via methods modified from previously published protocols for bladder<sup>19</sup> and myocardial matrix.<sup>8</sup> The decellularized pericardia (porcine and human) were lyophilized, ground into a coarse powder with a Wiley mini mill (Thomas Scientific, Swedesboro, NJ), and then frozen until further use. Milled samples were pepsin-digested in 0.1 M HCl at a concentration of 10 mg ECM per 1 mL HCl. Pepsin (Sigma, St. Louis, MO) was used at a concentration of 1 mg/mL. The ECM powder was digested for 60–65 h and neutralized to a pH of 7.4 with the addition of 1 M NaOH (1/10 of original digest volume) and 10 $\times$ PBS (1/10 of final neutralized volume). The neutralization step ceases pepsin activity; the enzyme is deactivated above pH 6.<sup>37</sup> All processing steps, including the pepsin digestion, were performed at room temperature. The resulting viscous solution, here called “solubilized ECM,” was diluted with 1 $\times$ PBS to the appropriate concentration.

### Characterization of solubilized ECM

One-dimensional gel electrophoresis was performed on human and porcine solubilized ECM (7 mg/mL) compared to rat tail collagen type I (2.5 mg/mL; BD Biosciences, San Jose, CA). The three solutions were run on a Tris-HCl, 12% polyacrylamide gel (Bio-Rad Laboratories, Hercules, CA) in

Tris/glycine/SDS buffer (Fisher Scientific, Hanover Park, IL), and 80 mM reducing agent dithiothreitol (Invitrogen, Carlsbad, CA). NuPAGE Plus2 Prestained Standard (1×) (Invitrogen) was used as the protein standard; all other samples were stained with Imperial Protein Stain (Pierce, Rockford, IL). Samples were prepared and run in an XCell Surelock MiniCell (Invitrogen). Glycosaminoglycan (GAG) content of the solubilized ECM was quantified using a colorimetric Blyscan GAG assay (Biocolor, Carrickfergus, United Kingdom). Samples were run in triplicate.

To more fully characterize the protein content of the solubilized ECM, tandem mass spectroscopy (MS/MS) was performed to identify the remaining proteins and peptide fragments. Solubilized ECM samples were briefly pepsin-digested before analysis by liquid chromatography (LC)-MS/MS with electrospray ionization, using a QSTAR-Elite hybrid mass spectrometer (Applied Biosciences, Foster City, CA) interfaced to a Tempo™ nanoscale reversed-phase high-pressure liquid chromatograph (Applied Biosciences) using a 10 cm 180 ID glass capillary packed with 5 μm C-18 Zorbax™ beads (Agilent Technologies, Santa Clara, CA). The buffer compositions were as follows: buffer A was composed of 98% H<sub>2</sub>O, 2% acetonitrile (ACN), 0.2% formic acid, and 0.005% trifluoroacetic acid (TFA); buffer B was composed of 100% acetonitrile (ACN), 0.2% formic acid, and 0.005% TFA. Peptides were eluted from the C-18 column into the mass spectrometer using a linear gradient of 5–60% buffer B over 60 min at 400 μL/min. LC-MS/MS data were acquired in a data-dependent fashion by selecting the four most intense peaks with charge state of two to four that exceeds 20 counts, with exclusion of former target ions set to 360 s and the mass tolerance for exclusion set to 100 ppm. MS/MS data were acquired from *m/z* 50 to 2000 Da by using “enhance all” and 24 time bins to sum, dynamic background subtract, automatic collision energy, and automatic MS/MS accumulation with the fragment intensity multiplier set to 6 and maximum accumulation set to 2 s before returning to the survey scan. Peptides were identified using paragon algorithm executed in Protein Pilot 2.0 (Life Technologies, Carlsbad, CA). Detected peptide sequences were run against the Swiss Prot databank for protein identification. Proteins were identified based on at least one peptide detected with a confidence of above 99% for that peptide identification. Additionally, a brief trypsin digest was performed on the solubilized ECM samples and the LC-MS/MS repeated as described. All mass spectroscopy work was performed at the Biomolecular Mass Spectroscopy Facility at the University of California, San Diego (La Jolla, CA).

#### Migration assay

Rat epicardial cells (RECs) (courtesy of Dr. David Bader) were cultured with Dulbecco's modified Eagle's medium (DMEM) with 10% fetal bovine serum (FBS) and 1% penicillin/streptomycin at 37°C with 5% CO<sub>2</sub>. These cells were grown on collagen-coated plates and split 1:4 before use. Passage 6 cells were used for this study. Human coronary artery endothelial cells (HCAECs) were purchased from Cell Applications (San Diego, CA), cultured with MesoEndo Cell Growth Medium (Cell Applications), and split 1:2 before use; passage 6 cells were used in this study. Rat aortic smooth muscle cells (RASMCs) were isolated as previously de-

scribed,<sup>8,38</sup> cultured with DMEM plus 10% FBS and 1% penicillin/streptomycin at 37°C with 5% CO<sub>2</sub>. These cells were grown on collagen-coated plates and split 1:4 before use, and passage 7 cells were used. Before use, all cell types were serum starved for 15 h in DMEM with 0.5% heat-inactivated FBS and 1% penicillin/streptomycin. A Chemotaxis 96-well Cell Migration Assay Kit (Chemicon, Billerica, MA) was used as previously described.<sup>39,40</sup> Four different chemoattractants were pipetted into the bottom well of a 96-well transwell plate: solubilized human pericardial ECM at 4 mg/mL, solubilized porcine pericardial ECM at 4 mg/mL, calf skin collagen type I at 4 mg/mL, and 10% FBS in DMEM. Both the solubilized ECM samples and the collagen were neutralized before use. RECs, RASMCs, and HCAECs were pipetted into the top chamber of the transwell plate and allowed to migrate toward the different solutions. Each condition was run in five to seven wells. After a 4-h incubation at 37°C and 5% CO<sub>2</sub>, the cells that had migrated through the membrane toward the bottom chamber were isolated, lysed, and stained with Cyquant dye per the manufacturer's protocol. To determine if the cells preferentially migrated toward a certain chemoattractant, fluorescence was read at 480/560 in a Spectramax plate reader. Relative fluorescent intensities correspond to relative number of cells that migrated through the membrane toward any given chemoattractant.

#### Myocardial injections

Solubilized human pericardium and porcine pericardium ECM were neutralized and diluted to 6.6 mg/mL. Myocardial injections were performed as previously described.<sup>8,9</sup> Briefly, 90 μL samples were drawn up into a syringe and injected into the LV-free wall of adult male Harlan Sprague-Dawley rats (375–400 g) through a 30-gauge needle. The animals were euthanized and the hearts excised at either 45 min (human, *n* = 2; porcine, *n* = 2) or at 14–15 days (human, *n* = 4; porcine, *n* = 6).

#### Histological and immunohistochemical analysis

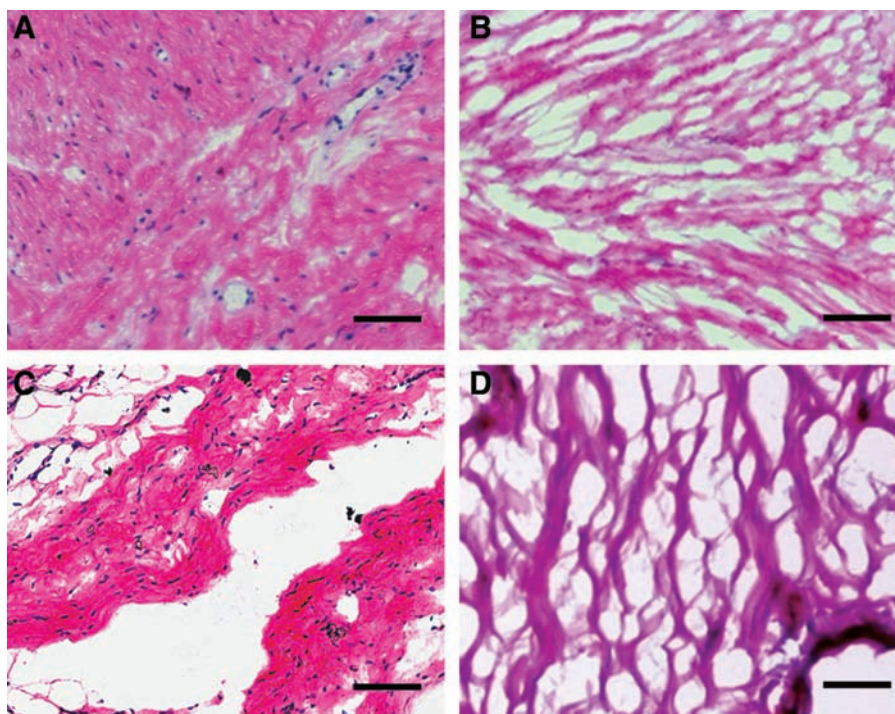
Hearts were fresh frozen, and short axis cross sections were taken every 400 μm from apex to base throughout each heart. Sections were fixed with acetone and stained with H&E for histological analysis. Sections were examined under a light microscope to locate the injection region and identify the two sections in which the injection region area was largest in each heart.

Immunohistochemistry was used to identify and quantify blood vessels that had formed in the injection region, as previously described.<sup>8</sup> Briefly, sections were costained with an anti-SMC antibody and fluorescein-isothiocyanate-labeled isolectin to identify smooth muscle and endothelial cells, respectively. The injection regions were outlined on the images and arterioles within the area were counted. c-Kit+ cells were also identified with a primary anti-c-Kit antibody (Santa Cruz Biotechnology, Santa Cruz, CA; 1:100 dilution), and with an AlexaFluor 468 goat anti-mouse secondary antibody (Invitrogen; 1:200 dilution).

#### Statistical analysis

A two-tailed Student's *t*-test was performed on the *in vivo* vessel ingrowth data; one-way analysis of variance was

**FIG. 1.** Histological analysis of pericardia. Hematoxylin and eosin (H&E) stains of (A) fresh human pericardium, (B) decellularized human pericardial matrix, (C) fresh porcine pericardium, and (D) decellularized porcine pericardial matrix. Scale bars: 500  $\mu$ m. Color images available online at [www.liebertonline.com/ten](http://www.liebertonline.com/ten).



performed for migration assay data with a Holm's corrected *t*-test. Statistical significance was accepted at  $p < 0.05$ . Values are reported as the mean  $\pm$  standard deviation.

## Results

### *Preparation of solubilized pericardial ECM*

Porcine and human pericardium samples were decellularized immediately upon collection, frozen, sectioned, and stained for analysis. Decellularization was first confirmed by histological analysis; H&E staining indicated an absence of nuclei as shown in Figure 1. A Hoechst 33342 stain for DNA

was then used to verify these results (data not shown). These two stains have been previously discussed as appropriate measures for determining decellularization.<sup>35,41</sup> For clinical relevance, we determined percent yield for each material, as an indication of tissue source feasibility. Lyophilization of a 2–4 cm<sup>2</sup> piece of porcine pericardium yields approximately 20 mg of dry-weight ECM; a similar-sized piece of human pericardium yields 17–40 mg of dry-weight ECM. Decellularized pericardium powder was solubilized with a pepsin digestion until the solution was visibly free of ECM particles, approximately 60–65 h. This process is illustrated in Figure 2, with examples of pericardium at each point: fresh (Fig. 2A),

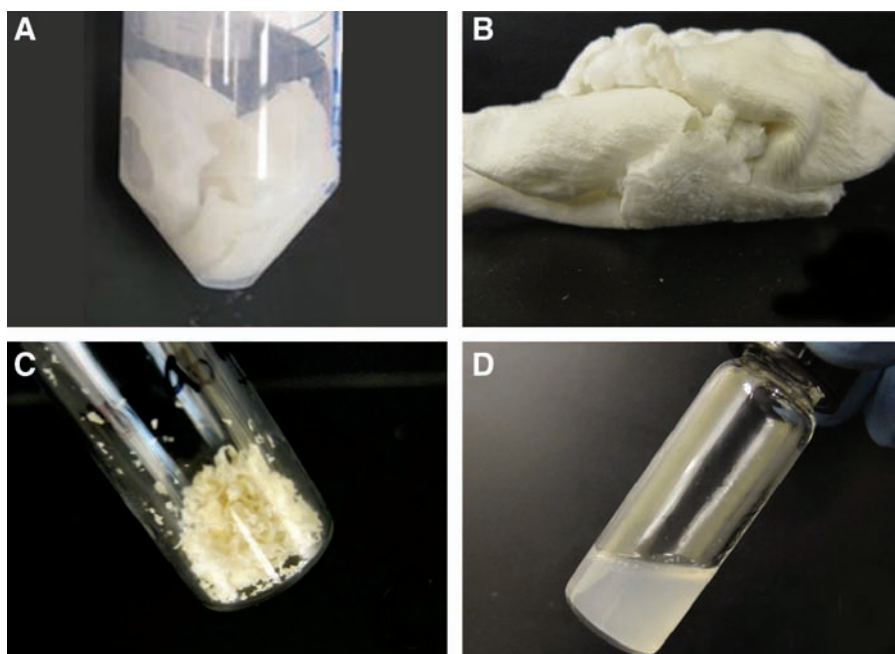


**FIG. 2.** Tissue processing. Decellularized porcine pericardium (A) was lyophilized (B), milled into a powder (C), and then solubilized (D). Color images available online at [www.liebertonline.com/ten](http://www.liebertonline.com/ten).

lyophilized (Fig. 2B), milled (Fig. 2C), and solubilized (Fig. 2D).

#### Characterization of solubilized pericardial ECM

Results of an SDS–polyacrylamide gel electrophoresis gel comparing the protein and peptide composition of solubi-

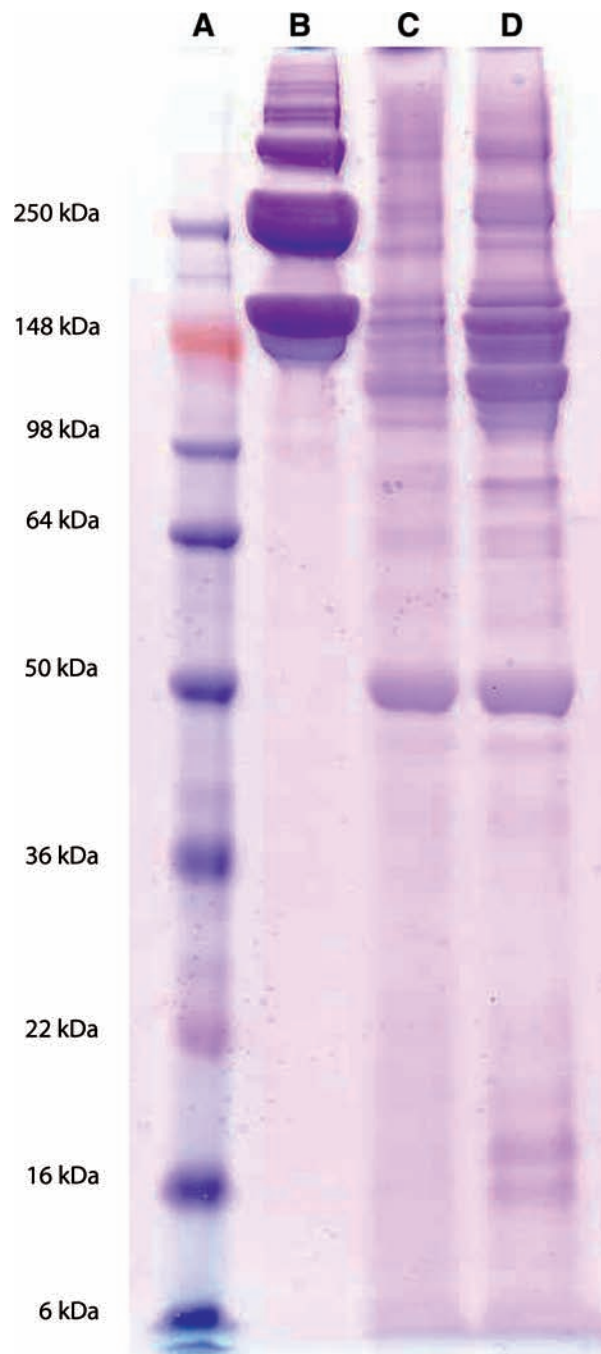


**FIG. 3.** Polyacrylamide gel electrophoresis results. (A) Molecular weight standard. (B) Rat tail collagen type I (2.5 mg/mL) compared to the solubilized human (C) and porcine (D) pericardial extracellular matrix (7 mg/mL). Note the presence of collagen as well as several other proteins/peptides in the pericardial matrix samples. Color images available online at [www.liebertonline.com/ten](http://www.liebertonline.com/ten).

lized human pericardial ECM (HPM), porcine pericardial ECM (PPM), and collagen indicate the presence of bands that match collagen in both pericardium samples, but also the presence of bands at lower molecular weights (Fig. 3). This composition was investigated further with mass spectroscopy, which identified fragments of a variety of ECM proteins, outlined in Table 1. The various types of collagen reported account for fibrillar, FACIT, basement membrane, and short-chain collagen, among others. Native pericardial ECM is primarily composed of collagen, elastin, and GAGs.<sup>26</sup> Peptide fragments derived from proteoglycans were also identified, namely, biglycan, which binds chondroitin or dermatan sulfate, lumican, and fibromodulin, which bind keratan sulfate, and FACIT collagen (type IX, XII, and XIV), which associates with various GAGs. Using the Blyscan assay, GAG content of the solubilized ECM was determined to be  $125.9 \pm 6.6$  and  $136.5 \pm 1.1$   $\mu\text{g}$  GAG per mg of dry ECM for the porcine and human samples, respectively.

#### In vitro migration assay

Results of the *in vitro* migration assay indicated that the porcine pericardium was the preferred chemoattractant for all three cell types investigated—RASMCs, RECs, and HCAECs ( $p < 0.05$ ). No cell type indicated a preference for the human pericardium over the positive control, FBS, which is a known chemoattractant for endothelial and smooth muscle cells.<sup>42,43</sup> The level of fluorescence reported in Figure 4 corresponds to the relative number of cells that have migrated through the transwell toward the different chemoattractants.

#### Myocardial injections

Solubilized pericardial ECM was injected into the LV-free wall of male Sprague-Dawley rats at a concentration of

**TABLE 1.** EXTRACELLULAR MATRIX COMPONENTS IDENTIFIED WITH MASS SPECTROSCOPY

Identified protein	HPM	PPM
Biglycan		X
Collagen type I	X	X
Collagen type II	X	X
Collagen type III	X	
Collagen type IV	X	X
Collagen type V		X
Collagen type VI		X
Collagen type VII		X
Collagen type VIII		X
Collagen type IX	X	
Collagen type X		X
Collagen type XI	X	X
Collagen type XII		X
Collagen type XIII		X
Collagen type XIV		X
Collagen type XXII	X	
Elastin	X	X
Fibrillin		X
Fibrinogen	X	
Fibromodulin		X
Lumican		X
Tropoelastin	X	X



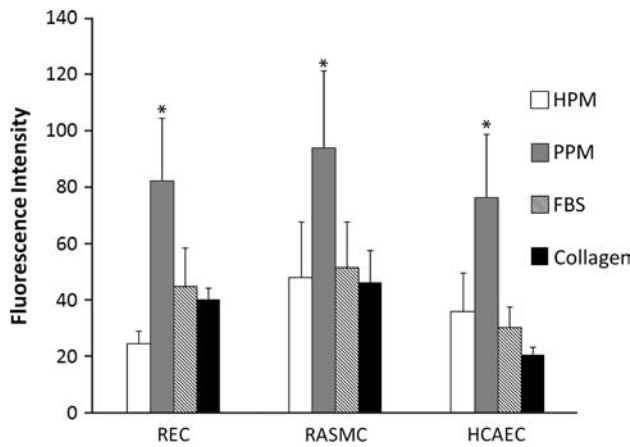


**FIG. 4.** *In vitro* migration assay. REC, RASMC, and HCAEC migration toward solubilized human pericardial matrix (HPM), porcine pericardial matrix (PPM), collagen, and 10% fetal bovine serum. Values are based on fluorescence data—intensity correlates to the number of cells that have migrated through the transwell membrane toward any given solution. \* $p < 0.05$  compared to other groups. REC, rat epicardial cell; RASMC, rat aortic smooth muscle cell; HCAEC, human coronary artery endothelial cell.

6.6 mg/mL. Both human and porcine pericardial ECM gelled within 45 min, the first time point at which hearts were excised for analysis. H&E sections (Fig. 5) show the area of gelled matrix *in vivo*—a fibrous, porous structure that gels interstitially, similar to findings reported for injected myocardial matrix.<sup>8</sup> Hearts were also collected after 2 weeks and examined for new vessel formation within the injection region. Representative images are presented in Figure 6, with smooth muscle cells labeled in red and endothelial cells in green. While the migration assay data indicated that the porcine pericardium was a stronger chemoattractant *in vitro*, results from these *in vivo* studies indicate that the porcine and human pericardial matrix gels have similar potential for promoting neovascularization. Hearts injected with human and porcine pericardial ECM gels showed statistically equivalent ( $p = 0.26$ ) number of arterioles after 2 weeks,  $76 \pm 13$  vessels per  $\text{mm}^2$  and  $51 \pm 42$  vessels per  $\text{mm}^2$ , respectively (Fig. 7).

Sections from the same injected hearts were also examined for the presence of stem cells, determined by a positive stain for c-Kit, a cluster of differentiation on the cell membrane of

hematopoietic stem cells shown to differentiate into myocardial precursors and vascular cells in the heart.<sup>44,45</sup> c-Kit+ cells were found within the injection region in clusters, identifiable by the fluorescent stain along the perimeter of the cells in Figure 8. This phenomenon occurred in very low numbers and thus was not quantified.

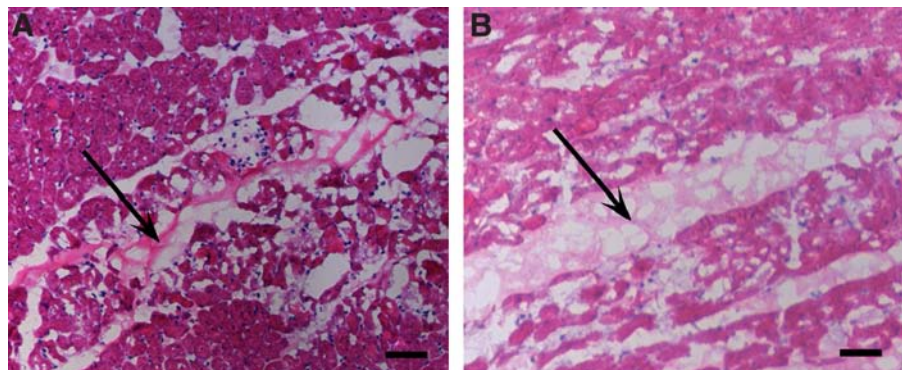
## Discussion

To overcome limited endogenous repair after ischemic injury in the myocardium and prevent the negative remodeling that leads to HF, a clinically relevant tissue engineering solution is needed. The ideal tissue-engineered scaffold would need to do the following: provide appropriate physical and biochemical cues, recruit cells to promote neovascularization and reduce fibrosis, and enhance the ability of resident and circulating stem cells to regenerate healthy cardiac tissue. Evidence of an increased number of cardiac progenitor cells present in damaged hearts<sup>44</sup> supports the understanding that regeneration could occur if the infarct environment were modified to be conducive to the recruitment, retention, and maturation of these cells.<sup>46</sup> Additionally, the ideal scaffold would be autologous and deliverable via minimally invasive methods.

Cardiac tissue engineering strategies have employed a diverse range of natural and synthetic materials, alone or in combination with various cell types, from skeletal myoblasts and cardiac fibroblasts to stem cells, in hopes of achieving regeneration.<sup>4–6,47,48</sup> What these materials attempt to provide is a three-dimensional microenvironment, or mimic of the ECM, to encourage myocardial regeneration. The native ECM is a complex, interconnected, and interdependent network of fibrous proteins, proteoglycans, GAGs, and other supporting molecules.<sup>27,49,50</sup> Its composition changes with age and plays a significant role in tissue development.<sup>51,52</sup> By providing the necessary microenvironment, the ECM plays a role in the regulation of many cellular activities, including migration and differentiation.<sup>49,50,53</sup> To fulfill these roles and promote a regenerative response, a tissue-engineered scaffold must be similarly capable of providing diverse biochemical cues. As such, the use of decellularized tissue-derived materials is attractive.

As functional materials, decellularized ECM scaffolds can encourage endogenous repair upon implantation or injection.<sup>27</sup> For example, cardiac patches made from small intestine submucosa and bladder matrix promote neovascularization and cell infiltration *in vivo*.<sup>7,32,33</sup> This effect is likely

**FIG. 5.** Myocardial injections: *in vivo* gelation. H&E stain of human (A) and porcine (B) pericardial matrix injections that have gelled *in vivo* after 45 min. Arrows denote matrix location, stained lighter pink than the myocardium. Scale bars: 500  $\mu\text{m}$ . Color images available online at [www.liebertonline.com/ten](http://www.liebertonline.com/ten).



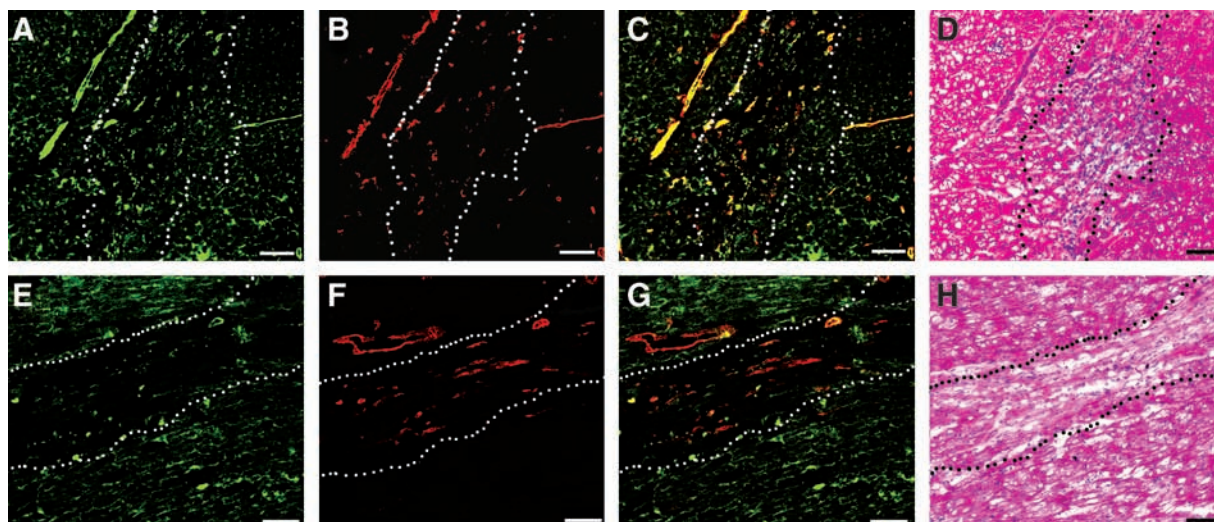


**FIG. 6.** Vasculature infiltration. Fluorescent stains for vessels in the injected human (A–C) and porcine (E–G) matrix gels at 2 weeks. Endothelial cells are labeled green (A, E), whereas smooth muscle cells are labeled red (B, F). Merged images are shown in (C) and (G). Scale bars: 100  $\mu\text{m}$ . The white or black dotted lines indicate the area of matrix injection, as determined by H&E analysis of a nearby section for both human (D) and porcine (H) matrix injections. Color images available online at [www.liebertonline.com/ten](http://www.liebertonline.com/ten).

enhanced by the biodegradable nature of tissue-derived scaffolds; degradation products of ECM components have been shown to have chemoattractive potential.<sup>39,50,54–57</sup> Moreover, collagen- and proteoglycan-derived fragments have been shown to be chemotactic for a variety of cell types.<sup>58–60</sup> Recently, decellularized cardiac ECM has been isolated,<sup>36,61,62</sup> allowing for a tissue-specific myocardial tissue engineering scaffold. An injectable form of cardiac ECM has also been shown to promote neovascularization and cell infiltration,<sup>8</sup> as previously found with other ECM sheets. A major limitation, however, shared by all of these decellularized materials is that they are typically derived from xenogenic or allogeneic sources. This raises concerns regarding

issues such as disease transfer and immunogenicity. For these reasons, among others, an autologous approach is more attractive from a clinical perspective. Using a patient's own tissue to produce a tissue engineering scaffold that elicits similar endogenous responses—specifically neovascularization and cellular infiltration—would provide a faster route to clinical translation.

With these guidelines in mind, the pericardium was investigated for its potential as an injectable tissue engineered scaffold for cardiac repair. Similar to the other matrix materials discussed, decellularized sheets of porcine pericardium have been shown to promote endothelial cell infiltration *in vitro*.<sup>63,64</sup> Pericardial tissue is a commonly used biomaterial and has been shown to be especially useful for valve replacements<sup>22</sup> and wound healing applications<sup>65,66</sup>; thus, it was a strong candidate for development as an injectable scaffold for cardiac repair. The investigation of pericardial tissue is of great clinical interest because human pericardium can be surgically resected without adverse consequences and is therefore a potential source for an autologous scaffold. The protocol and techniques described herein were first established with porcine tissue collected from young, healthy, farm pigs—a common source of xenogenic tissue used in applications of decellularized material. When it was determined that an injectable matrix gel made from porcine pericardium would gel *in situ* and promote neovascularization upon injection in the LV-free wall, we next investigated human pericardium, since it has the distinct advantage of being potentially autologous.

Characterization of the two gels by mass spectroscopy identified an array of collagen and elastin proteins, as well as supporting ECM proteins such as fibrillin and fibrinogen, indicating that, even after processing, the solubilized pericardial matrix retains a high degree of fidelity to the original ECM composition. While the composition of the pericardial ECM is similar in the porcine and human specimens, the former was collected from young, healthy animals, whereas

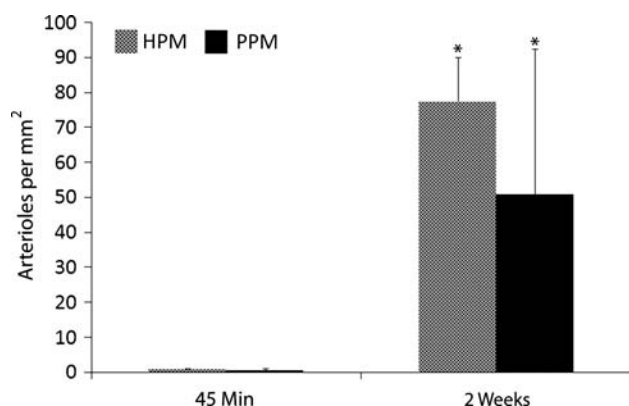
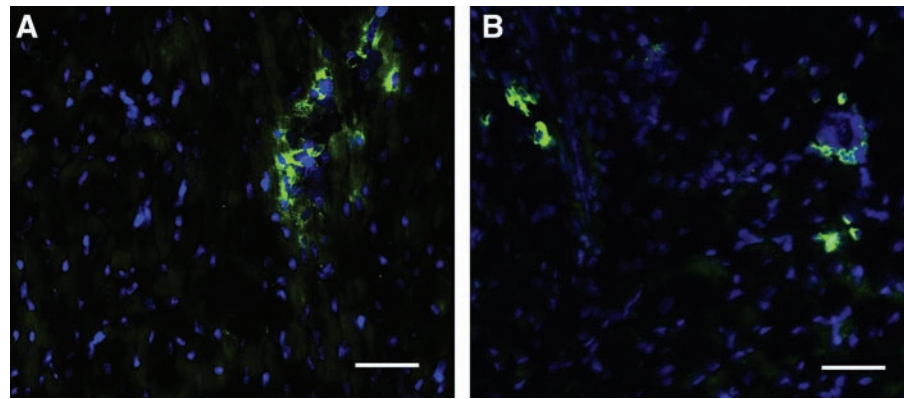


**FIG. 7.** Quantification of arteriole density in matrix injection regions. Injection of human and porcine pericardial matrix caused a neovascularization response that was quantified by the increase in the average number of vessels with average diameters greater than 10  $\mu\text{m}$  per  $\text{mm}^2$  of injection region after 2 weeks compared to 45 min ( $*p < 0.01$ ). The two materials caused a statistically similar response ( $p = 0.26$ ).



**FIG. 8.** Stem cells within matrix injection region. A Hoechst stain for nuclei (blue) and an immunohistochemical stain for c-kit (green) identifies stem cells in the human (A) and porcine (B) matrix injection regions. Scale bars: 50  $\mu$ m. Color images available online at [www.liebertonline.com/ten](http://www.liebertonline.com/ten).



the latter was donated by significantly older, diseased individuals; it was thus hypothesized that these differences may reduce the chemoattractive potential and regenerative capacity of the human tissue. The results of the *in vitro* migration assay supported this hypothesis—all cell types preferentially migrated toward the porcine pericardial matrix, whereas no increase in migration was seen toward the human pericardial matrix with respect to the positive control, FBS. *In vivo*, however, the two materials performed similarly—the human pericardial matrix gel allowed for comparable vessel ingrowth. This is potentially due to a slight inflammatory response as a result of injection injury, the structural properties of the gelled matrix that encouraged cell infiltration—as other fibrous, porous, three-dimensional scaffolds have performed similarly,<sup>67,68</sup>—and other complex *in vivo* conditions not represented in the *in vitro* assay.

Clinical relevance of this material was evaluated by an array of considerations, including percent yield, induction of neovascularization *in vivo*, and ease of clinical translation. When determining percent yield, or what injection volume could be produced from a small (<4 cm<sup>2</sup>) piece of pericardium, this tissue size was found to be sufficient for 3 mL of injections, indicating feasibility for treating an MI. As discussed, both materials allow for cellular infiltration and arteriole formation within 2 weeks. With respect to ease of translation, decellularized porcine pericardium is already FDA approved for use in humans and has a well-established history as a biomaterial. As a potentially autologous avenue, human pericardium can be surgically resected without adverse consequences; thoracoscopic pericardiectomy is a minimally invasive procedure for removal of the pericardium. It should be noted that while pericardial tissue comprises the functional portion of the pericardial matrix gel, for a fully autologous therapy, the pepsin used to solubilize the matrix should likewise be autologous. To this end, pepsin can be isolated in relevant quantities from patient gastric juice collected via nasogastric aspiration,<sup>69</sup> thereby ensuring that all biological components are autologous. The material developed here could be administered as an acellular scaffold, or in conjunction with cells such as adult stem cells, induced pluripotent stem cells, or other autologous cell types.

Thus, proof of concept has been established for the use of these matrix gels for cardiac repair. Porcine and human pericardial ECM gels were shown to be injectable and therefore potentially deliverable via currently used, mini-

mally invasive methods, to promote neovascularization *in vivo*, and to allow for stem cell infiltration. With clinical translation as the ultimate goal, the pericardium is a strong candidate for cardiac tissue engineering since it has potential to be an autologous therapy.

### Conclusions

With these findings, we have demonstrated proof of concept for the use of decellularized pericardial matrix gels as injectable scaffolds for the myocardium. Results of characterization assays indicate that matrix gels produced from decellularized pericardium retained native ECM components, including GAGs, and *in vitro* migration assay results demonstrate the potential of porcine pericardial matrix to serve as a chemoattractant for relevant cell types—epicardial, endothelial, and smooth muscle cells. Further, *in vivo* studies show the two materials allow for comparable degrees of vascular cell infiltration and arteriole formation at 2 weeks, thus demonstrating feasibility as an injectable treatment. c-Kit<sup>+</sup> cells were also found within the injection region, indicating the potential for stem cell migration into the matrix material. Sacrificing tissue specificity for the possibility of an autologous therapy, the pericardium is identified as a source of patient-specific ECM for the production of an injectable scaffold for the myocardium.

### Acknowledgments

The authors would like to acknowledge Dr. Michael Madani and Dr. Kirk Knowlton for their help in procuring human tissue samples, Dr. Majid Ghassemian for assistance with mass spectroscopy data, Carolina Rogers for her guidance and cooperation in the harvesting of porcine specimens, Cynthia Cam for assistance with biochemical assays, and Dana Rutherford for assistance with immunohistochemistry. This research was supported in part by the NIH Director's New Innovator Award Program, part of the NIH Roadmap for Medical Research, through grant number 1-DP2-OD004309-01. S.B.S.-N. would like to thank the NSF for a Graduate Research Fellowship.

### Disclosure Statement

The authors have no competing financial interests to disclose.



## References

- Lloyd-Jones, D., Adams, R., Carnethon, M., De Simone, G., Ferguson, T.B., Flegal, K., Ford, E., Furie, K., Go, A., Greenlund, K., Haase, N., Hailpern, S., Ho, M., Howard, V., Kissela, B., Kittner, S., Lackland, D., Lisabeth, L., Marelli, A., McDermott, M., Meigs, J., Mozaffarian, D., Nichol, G., O'Donnell, C., Roger, V., Rosamond, W., Sacco, R., Sorlie, P., Stafford, R., Steinberger, J., Thom, T., Wasserthiel-Smoller, S., Wong, N., Wylie-Rosett, J., Hong, Y.; American Heart Association Statistics Committee and Stroke Statistics Subcommittee. Heart Disease and Stroke Statistics—2009 Update: A report from the American Heart Association Statistics Committee and Stroke Statistics Subcommittee. *Circulation* **119**, e21, 2009.
- Bergmann, O., Bhardwaj, R.D., Bernard, S., Zdunek, S., Barnabe-Heider, F., Walsh, S., Zupicich, J., Alkass, K., Buchholz, B.A., Druid, H., Jovinge, S., and Frisen, J. Evidence for cardiomyocyte renewal in humans. *Science* **324**, 98, 2009.
- Mann, D.L. Mechanisms and models in heart failure: a combinatorial approach. *Circulation* **100**, 999, 1999.
- Laflamme, M.A., and Murry, C.E. Regenerating the heart. *Nat Biotechnol* **23**, 845, 2005.
- Reffellmann, T., and Kloner, R.A. Cellular cardiomyoplasty—cardiomyocytes, skeletal myoblasts, or stem cells for regenerating myocardium and treatment of heart failure? *Cardiovasc Res* **58**, 358, 2003.
- Christman, K.L., and Lee, R.J. Biomaterials for the treatment of myocardial infarction. *J Am Coll Cardiol* **48**, 907, 2006.
- Martinez, E.C., and Kofidis, T. Myocardial tissue engineering: the quest for the ideal myocardial substitute. *Expert Rev Cardiovasc Ther* **7**, 921, 2009.
- Singelyn, J.M., DeQuach, J.A., Seif-Naraghi, S.B., Littlefield, R.B., Schup-Magoffin, P.J., and Christman, K.L. Naturally derived myocardial matrix as an injectable scaffold for cardiac tissue engineering. *Biomaterials* **30**, 5409, 2009.
- Christman, K.L., Vardanian, A.J., Fang, Q., Sievers, R.E., Fok, H.H., and Lee, R.J. Injectable fibrin scaffold improves cell transplant survival, reduces infarct expansion, and induces neovasculature formation in ischemic myocardium. *J Am Coll Cardiol* **44**, 654, 2004.
- Christman, K.L., Fok, H.H., Sievers, R.E., Fang, Q., and Lee, R.J. Fibrin glue alone and skeletal myoblasts in a fibrin scaffold preserve cardiac function after myocardial infarction. *Tissue Eng* **10**, 403, 2004.
- Huang, N.F., Yu, J., Sievers, R., Li, S., and Lee, R.J. Injectable biopolymers enhance angiogenesis after myocardial infarction. *Tissue Eng* **11**, 1860, 2005.
- Landa, N., Miller, L., Feinberg, M.S., Holbova, R., Shachar, M., Freeman, I., Cohen, S., and Leor, J. Effect of injectable alginate implant on cardiac remodeling and function after recent and old infarcts in Rat. *Circulation* **117**, 1388, 2008.
- Lu, W.N., Lu, S.H., Wang, H.B., Li, D.X., Duan, C.M., Liu, Z.Q., Hao, T., He, W.J., Xu, B., Fu, Q., Song, Y.C., Xie, X.H., and Wang, C.Y. Functional improvement of infarcted heart by co-injection of embryonic stem cells with temperature-responsive chitosan hydrogel. *Tissue Eng Part A* **15**, 1437, 2009.
- Davis, M.E., Motion, J.P., Narmoneva, D.A., Takahashi, T., Hakuno, D., Kamm, R.D., Zhang, S., and Lee, R.T. Injectable self-assembling peptide nanofibers create intramyocardial microenvironments for endothelial cells. *Circulation* **111**, 442, 2005.
- Hsieh, P.C., Davis, M.E., Gannon, J., MacGillivray, C., and Lee, R.T. Controlled delivery of PDGF-BB for myocardial protection using injectable self-assembling peptide nanofibers. *J Clin Invest* **116**, 237, 2006.
- Padin-Iruegas, M.E.M.D., Misao, Y.M.D., Davis, M.E.P., Segers, V.F.M.M.D.P., Esposito, G.P., Tokunou, T.M.D.P., Urbanek, K.M.D., Hosoda, T.M.D.P., Rota, M.P., Anversa, P.M.D., Leri, A.M.D., Lee, R.T.M.D., and Kajstura, J.P. Cardiac progenitor cells and biotinylated insulin-like growth factor-1 nanofibers improve endogenous and exogenous myocardial regeneration after infarction. *Circulation* **120**, 876, 2009.
- Dobner, S., Bezuidenhout, D., Govender, P., Zilla, P., and Davies, N. A synthetic non-degradable polyethylene glycol hydrogel retards adverse post-infarct left ventricular remodeling. *J Card Fail* **15**, 629, 2009.
- Kofidis, T., Lebl, D.R., Martinez, E.C., Hoyt, G., Tanaka, M., and Robbins, R.C. Novel injectable bioartificial tissue facilitates targeted, less invasive, large-scale tissue restoration on the beating heart after myocardial injury. *Circulation* **112**, I173, 2005.
- Freytes, D.O., Martin, J., Velankar, S.S., Lee, A.S., and Badylak, S.F. Preparation and rheological characterization of a gel form of the porcine urinary bladder matrix. *Biomaterials* **29**, 1630, 2008.
- Colombo, A., Almagor, Y., Gaspar, J., and Vonderwalde, C. The pericardium covered stent (PCS). *EuroIntervention* **5**, 394, 2009.
- Baharuddin, A., Go, B.T., Firdaus, M.N., and Abdullah, J. Bovine pericardium for dural graft: clinical results in 22 patients. *Clin Neurol Neurosurg* **104**, 342, 2002.
- Rahimtoola, S.H. Choice of prosthetic heart valve for adult patients. *J Am Coll Cardiol* **41**, 893, 2003.
- Hvass, U., and O'Brien, M.F. The stentless Cryolife-O'Brien aortic porcine xenograft: a five-year follow-up. *Ann Thorac Surg* **66**, S134, 1998.
- Garlick, R.B., and O'Brien, M.F. The CryoLife-O'Brien composite stentless porcine aortic xenograft valve in 118 patients. *Jpn Circ J* **61**, 682, 1997.
- O'Brien, M.F. The Cryolife-O'Brien composite aortic stentless xenograft: surgical technique of implantation. *Ann Thorac Surg* **60**, S410, 1995.
- Braga-Vilela, A.S., Pimentel, E.R., Marangoni, S., Toyama, M.H., and de Campos Vidal, B. Extracellular matrix of porcine pericardium: biochemistry and collagen architecture. *J Membr Biol* **221**, 15, 2008.
- Badylak, S.F. The extracellular matrix as a biologic scaffold material. *Biomaterials* **28**, 3587, 2007.
- Fuster, V. *Hurst's the heart*. New York: McGraw-Hill Medical Publishing Division, 2001.
- Duran, C.M., Gometza, B., Kumar, N., Gallo, R., and Martin-Duran, R. Aortic valve replacement with freehand autologous pericardium. *J Thorac Cardiovasc Surg* **110**, 511, 1995.
- Chauvaud, S., Jebara, V., Chachques, J.C., el Asmar, B., Mihaileanu, S., Perier, P., Dreyfus, G., Relland, J., Couetil, J.P., and Carpentier, A. Valve extension with glutaraldehyde-preserved autologous pericardium. Results in mitral valve repair. *J Thorac Cardiovasc Surg* **102**, 171, 1991.
- David, T.E., Feindel, C.M., and Ropchan, G.V. Reconstruction of the left ventricle with autologous pericardium. *J Thorac Cardiovasc Surg* **94**, 710, 1987.
- Badylak, S., Obermiller, J., Geddes, L., and Matheny, R. Extracellular matrix for myocardial repair. *Heart Surg Forum* **6**, E20, 2003.

33. Robinson, K.A., Li, J., Mathison, M., Redkar, A., Cui, J., Chronos, N.A., Matheny, R.G., and Badylak, S.F. Extracellular matrix scaffold for cardiac repair. *Circulation* **112**, 1135, 2005.
34. Mirsadraee, S., Wilcox, H.E., Korossis, S.A., Kearney, J.N., Watterson, K.G., Fisher, J., and Ingham, E. Development and characterization of an acellular human pericardial matrix for tissue engineering. *Tissue Eng* **12**, 763, 2006.
35. Gilbert, T.W., Sellaro, T.L., and Badylak, S.F. Decellularization of tissues and organs. *Biomaterials* **27**, 3675, 2006.
36. Eitan, Y., Sarig, U., Dahan, N., and Machluf, M. Acellular cardiac extracellular matrix as a scaffold for tissue engineering: *in-vitro* cell support, remodeling and biocompatibility. *Tissue Eng Part C Methods* 2009. (In press).
37. Johnston, N., Dettmar, P.W., Bishwokarma, B., Lively, M.O., and Koufman, J.A. Activity/stability of human pepsin: implications for reflux attributed laryngeal disease. *Laryngoscope* **117**, 1036, 2007.
38. San Antonio, J.D., Karnovsky, M.J., Ottlinger, M.E., Schilling, R., and Pukac, L.A. Isolation of heparin-insensitive aortic smooth muscle cells. Growth and differentiation. *Arterioscler Thromb* **13**, 748, 1993.
39. Reing, J.E., Zhang, L., Myers-Irvin, J., Cordero, K.E., Freytes, D.O., Heber-Katz, E., Bedelbaeva, K., McIntosh, D., Dewilde, A., Brauhut, S.J., and Badylak, S.F. Degradation products of extracellular matrix affect cell migration and proliferation. *Tissue Eng Part A* **15**, 605, 2009.
40. Akahane, T., Akahane, M., Shah, A., Connor, C.M., and Thorgeirsson, U.P. TIMP-1 inhibits microvascular endothelial cell migration by MMP-dependent and MMP-independent mechanisms. *Exp Cell Res* **301**, 158, 2004.
41. Badylak, S.F., and Gilbert, T.W. Immune response to biologic scaffold materials. *Semin Immunol* **20**, 109, 2008.
42. Di Luozzo, G., Pradhan, S., Dhadwal, A.K., Chen, A., Ueno, H., and Sumpio, B.E. Nicotine induces mitogen-activated protein kinase dependent vascular smooth muscle cell migration. *Atherosclerosis* **178**, 271, 2005.
43. Lau, Y.T., and Ma, W.C. Nitric oxide inhibits migration of cultured endothelial cells. *Biochem Biophys Res Commun* **221**, 670, 1996.
44. Beltrami, A.P., Barlucchi, L., Torella, D., Baker, M., Limana, F., Chimenti, S., Kasahara, H., Rota, M., Musso, E., Urbanek, K., Leri, A., Kajstura, J., Nadal-Ginard, B., and Anversa, P. Adult cardiac stem cells are multipotent and support myocardial regeneration. *Cell* **114**, 763, 2003.
45. Limana, F., Zacheo, A., Mocini, D., Mangoni, A., Borsellino, G., Diamantini, A., De Mori, R., Battistini, L., Vigna, E., Santini, M., Loiaconi, V., Pompilio, G., Germani, A., and Capogrossi, M.C. Identification of myocardial and vascular precursor cells in human and mouse epicardium. *Circ Res* **101**, 1255, 2007.
46. Kubo, H., Jaleel, N., Kumarapeli, A., Berretta, R.M., Bratinov, G., Shan, X., Wang, H., Houser, S.R., and Margulies, K.B. Increased cardiac myocyte progenitors in failing human hearts. *Circulation* **118**, 649, 2008.
47. Etzion, S., Barbash, I.M., Feinberg, M.S., Zarin, P., Miller, L., Guetta, E., Holbova, R., Kloner, R.A., Kedes, L.H., and Leor, J. Cellular cardiomyoplasty of cardiac fibroblasts by adenoviral delivery of MyoD *ex vivo*: an unlimited source of cells for myocardial repair. *Circulation* **106**, I, 2002.
48. Kao, R.L., Browder, W., and Li, C. Cellular cardiomyoplasty: what have we learned? *Asian Cardiovasc Thorac Ann* **17**, 89, 2009.
49. Leor, J., Amsalem, Y., and Cohen, S. Cells, scaffolds, and molecules for myocardial tissue engineering. *Pharmacol Ther* **105**, 151, 2005.
50. Lutolf, M.P., and Hubbell, J.A. Synthetic biomaterials as instructive extracellular microenvironments for morphogenesis in tissue engineering. *Nat Biotechnol* **23**, 47, 2005.
51. Brown, L. Cardiac extracellular matrix: a dynamic entity. *Am J Physiol Heart Circ Physiol* **289**, H973, 2005.
52. Francesco, R., Antonio, G., Manlio, B., and Alfonso, B. From cell-ECM interactions to tissue engineering. *J Cell Physiol* **199**, 174, 2004.
53. Uriel, S., Labay, E., Francis-Sedlak, M., Moya, M.L., Weichselbaum, R.R., Ervin, N., Cankova, Z., and Brey, E.M. Extraction and assembly of tissue-derived gels for cell culture and tissue engineering. *Tissue Eng Part C Methods* **15**, 309, 2009.
54. Beattie, A.J., Gilbert, T.W., Guyot, J.P., Yates, A.J., and Badylak, S.F. Chemoattraction of progenitor cells by remodeling extracellular matrix scaffolds. *Tissue Eng Part A* **15**, 1119, 2009.
55. Brennan, E.P., Tang, X.H., Stewart-Akers, A.M., Gudas, L.J., and Badylak, S.F. Chemoattractant activity of degradation products of fetal and adult skin extracellular matrix for keratinocyte progenitor cells. *J Tissue Eng Regen Med* **2**, 491, 2008.
56. Sarikaya, A., Record, R., Wu, C.C., Tullius, B., Badylak, S., and Ladisch, M. Antimicrobial activity associated with extracellular matrices. *Tissue Eng* **8**, 63, 2002.
57. Brennan, E.P., Reing, J., Chew, D., Myers-Irvin, J.M., Young, E.J., and Badylak, S.F. Antibacterial activity within degradation products of biological scaffolds composed of extracellular matrix. *Tissue Eng* **12**, 2949, 2006.
58. Isoda, M. Eosinophil chemotactic activity of collagen-derived fragments—a preliminary report. *J Dermatol* **15**, 83, 1988.
59. Mundy, G.R., DeMartino, S., and Rowe, D.W. Collagen and collagen-derived fragments are chemotactic for tumor cells. *J Clin Invest* **68**, 1102, 1981.
60. Moore, A.R., Chander, C.L., Hanahoe, T.H., Howat, D.W., Desa, F.M., Colville-Nash, P.R., and Willoughby, D.A. The chemotactic properties of cartilage glycosaminoglycans for polymorphonuclear neutrophils. *Int J Tissue React* **11**, 301, 1989.
61. Ott, H.C., Matthiesen, T.S., Goh, S.K., Black, L.D., Kren, S.M., Netoff, T.I., and Taylor, D.A. Perfusion-decellularized matrix: using nature's platform to engineer a bioartificial heart. *Nat Med* **14**, 213, 2008.
62. Wainwright, J.M., Czajka, C.A., Patel, U.B., Freytes, D.O., Tobita, K., Gilbert, T.W., and Badylak, S.F. Preparation of cardiac extracellular matrix from an intact porcine heart. *Tissue Eng Part C Methods* 2009. (In press).
63. Li, F., Li, W., Johnson, S., Ingram, D., Yoder, M., and Badylak, S. Low-molecular-weight peptides derived from extracellular matrix as chemoattractants for primary endothelial cells. *Endothelium* **11**, 199, 2004.
64. Bader, A., Schilling, T., Teebken, O.E., Brandes, G., Herden, T., Steinhoff, G., and Haverich, A. Tissue engineering of heart valves—human endothelial cell seeding of detergent acellularized porcine valves. *Eur J Cardiothorac Surg* **14**, 279, 1998.
65. Hodde, J. Naturally occurring scaffolds for soft tissue repair and regeneration. *Tissue Eng* **8**, 295, 2002.
66. Landsman, A., Taft, D., and Riemer, K. The role of collagen bioscaffolds, foamed collagen, and living skin

- equivalents in wound healing. *Clin Podiatr Med Surg* **26**, 525, 2009.
67. Lai, P.H., Chang, Y., Chen, S.C., Wang, C.C., Liang, H.C., Chang, W.C., and Sung, H.W. Acellular biological tissues containing inherent glycosaminoglycans for loading basic fibroblast growth factor promote angiogenesis and tissue regeneration. *Tissue Eng* **12**, 2499, 2006.
68. Nam, J., Huang, Y., Agarwal, S., and Lannutti, J. Improved cellular infiltration in electrospun fiber via engineered porosity. *Tissue Eng* **13**, 2249, 2007.
69. Roberts, N.B., and Taylor, W.H. The preparation and purification of individual human pepsins by using diethylaminoethyl-cellulose. *Biochem J* **169**, 607, 1978.

Address correspondence to:  
Karen L. Christman, Ph.D.  
Department of Bioengineering  
University of California, San Diego  
9500 Gilman Drive  
La Jolla, CA 92093-0412

E-mail: christman@bioeng.ucsd.edu

Received: November 30, 2009  
Accepted: January 22, 2010  
Online Publication Date: February 25, 2010



